Calculation of resonant states for double Coulomb acceptor in narrow-gap HgCdTe

© M.S. Zholudev, D.V. Kozlov, S.V. Morozov

Institute of Physics of Microstructures, Russian Academy of Sciences,
603950 Nizhny Novgorod, Russia
Lobachevsky State University,
603950 Nizhny Novgorod, Russia

E-mail: zholudev@ipmras.ru

Received August 24, 2023
Revised September 1, 2023
Accepted September 1, 2023

Localized and resonant state energies of double Coulomb acceptor in narrow-gap HgCdTe alloys are calculated. The simulation is made with scattering matrix technique within spherically symmetric three-band Kane model taking into account conduction band and two top valence bands. It is shown that appearance one-particle state is highly unlikely when the two-particle state is resonant.

Keywords: double acceptor, resonant states, mercury cadmium telluride.

DOI: 10.61011/SC.2023.06.57162.37k

1. Introduction

A solid solution of cadmium-mercury-tellurium (CMT) attracts the constant interest of researchers due to a number of specific fundamental effects [1–4] and the possibilities of application in the field of infrared optoelectronics [5], including the prospect of creating laser diodes [6,7]. This material owes its outstanding properties to the peculiarities of the zone structure. The bottom of the conduction band in CdTe is formed by wave functions with symmetry Γ_6, and the ceiling of the valence band — by wave functions with symmetry Γ_8. The width of the band gap at low temperatures in this material is ~ 1.6 eV. The HgTe semiconductor has an inverted band structure, in which the bottom of the conduction band and the ceiling of the valence band are formed by wave functions with symmetry Γ_8, and the zone with symmetry Γ_6 is located at ~ 0.3 eV lower in energy. Therefore, it is sometimes said that this material has a negative band gap. In fact, mercury telluride is slit-free, since due to the same symmetry of the wave functions of the conduction band and the valence band, a violation of the symmetry of the crystal, for example, uniaxial deformation, is required to remove the degeneracy at the point of their contact. Thus, depending on the composition of the solid solution, a material with an inverted or normal band structure with a band gap from 0.3 to 1.6 eV can be obtained.

When studying the properties of this material in the mid-infrared and terahertz ranges, impurity states play an important role. In particular, mercury vacancies that arise due to the high degree of segregation of Hg atoms are a natural acceptor for CMT. This defect is divalent, i. e. in a fully ionized state it has a charge of $-2e$. Resonant states occur in narrow-band and gap-free materials, where the band gap width is less than the ionization energy of the acceptors. These levels lead to the appearance of features in the spectra that are clearly visible against the background of the corresponding interband transitions. Such lines attributed to mercury vacancies [8] have already been observed experimentally in the CMT [9].

Significant progress has recently been made in the theoretical study of the discrete spectrum of mercury vacancies [8,10]. However, modeling of resonant states was complicated by the need to solve unstable equations for wave functions of a continuous spectrum [11]. The calculation method developed for such problems based on the scattering matrix was successfully used earlier to study localized and resonant states of single-charge acceptors [12–14], and it is used in this paper to describe a two-charge Coulomb acceptor. The study of this model, which does not require fitting parameters, is a natural preliminary step for studying the structure of resonant states of mercury vacancies, since it allows us to draw a number of qualitative conclusions.

2. Calculation method

When describing acceptor states, a „hole“ band structure is often used, in which the valence band is located on top and has a positive mass. However, when studying resonant states in the conduction band, as well as interband transitions, the „electronic“ band structure is more convenient. At the same time, however, it should be borne in mind that purely electronic formalism is suitable only for the qualitative description of acceptor states and transitions. For a quantitative study of such a system, it is necessary to use the concept of a hole as a quasi-particle, which is a perturbation of the electron distribution in the valence band.

Three types of [10] states are characteristic of a two-charge acceptor: doubly ionized (A_2^{-2}), once ionized (A_2^{-1}) and neutral (A_2^0). It is necessary to understand what the

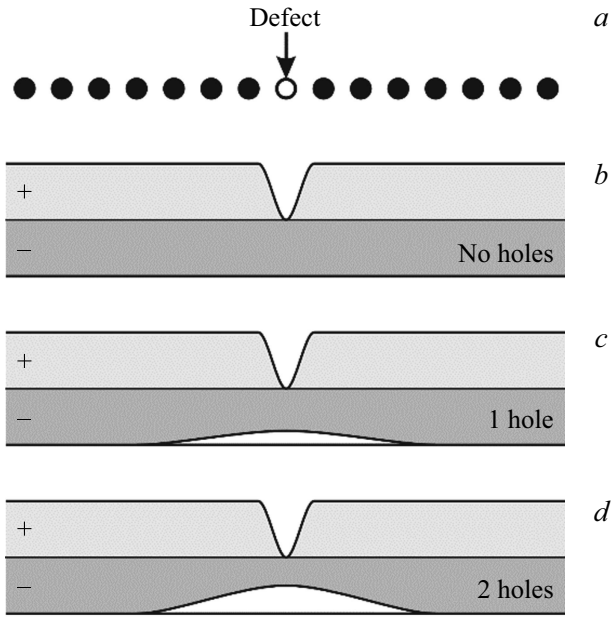

Figure 1. Charge density distribution scheme in various states of a divalent acceptor: *a* — location of the defect; *b* — fully ionized acceptor; *c* — once ionized acceptor; *d* — neutral acceptor. The signs „+“ and „−“ indicate the charge density created by ions and electrons, respectively.

defect potential is in each of the three cases for calculating the energies and wave functions of carriers in these states. Since the acceptor is a defect in the crystal lattice, its potential, of course, is the difference between the potential of a crystal with a defect and without it. In the case of a divalent Coulomb acceptor, this potential is equal to the potential of a double negative point charge:

$$\varphi_0(\mathbf{r}) = \frac{2e}{\epsilon_0 r}. \qquad (1)$$

The total potential acting on an electron consists of the field of ions and the field of other electrons. If the electron distribution is uniform, as in an ideal crystal (Figure 1, *b*), then the defect field is not compensated, and the total potential will be determined by the expression (1). This corresponds to the case of a doubly ionized acceptor A_2^{-2}.

Since the mass of electrons in the valence band is negative, the repulsive potential (1) will create localized states near the defect, the energy of which will be higher than the ceiling of the valence band. These levels should be interpreted as hole levels, i. e. the wave function of the deepest state — is the wave function of the hole that will arise after the departure of one electron from the region of the repulsive potential (Figure 1, *c*). The resulting structure is a single ionized acceptor A_2^{-1}. The energy released when the first electron leaves and the wave function of the resulting hole obey the Schrodinger equation with potential (1):

$$\big(\hat{H}_0 + e\varphi_0(\mathbf{r})\big)\psi_0(\mathbf{r}) = E_0\psi_0(\mathbf{r}). \qquad (2)$$

In the case A_2^{-1} of the center, its field consists of the potential of a fully ionized acceptor (1) and the potential of the first captured hole, which satisfies the Poisson equation:

$$\Delta\varphi(\mathbf{r}) = -\frac{4\pi e}{\epsilon_0}|\psi_0(\mathbf{r})|^2.$$

This potential is still repulsive and can provoke the departure of another electron, which is equivalent to the capture of a second hole with the formation of a A_2^0-center. The second hole, in turn, will affect the first one and change its state so that it will differ from the solution of equation (2). Both holes are identical and therefore must have the same energies and wave functions (this is possible since the ground state of the acceptor is fourfold degenerated). Thus, the energy and wave function of each of the particles must satisfy a self-consistent system of Schrodinger–Poisson equations:

$$\big(\hat{H}_0 + e\varphi_0(\mathbf{r}) + e\varphi_h(\mathbf{r})\big)\psi_h(\mathbf{r}) = E_h\psi_h(\mathbf{r}), \qquad (3)$$

$$\Delta\varphi_h(\mathbf{r}) = -\frac{4\pi e}{\epsilon_0}|\psi_h(\mathbf{r})|^2. \qquad (4)$$

System of equations (3) and (4) were solved iteratively using the following recursive equations:

$$\varphi_{h,0}(\mathbf{r}) = 0,$$

$$\big(\hat{H}_0 + e\varphi_0(\mathbf{r}) + e\varphi_{h,i}(\mathbf{r})\big)\psi_{h,i}(\mathbf{r}) = E_{h,i}\psi_{h,i}(\mathbf{r}),$$

$$\Delta\varphi_{h,i+1}(\mathbf{r}) = -\frac{4\pi e}{\epsilon_0}|\psi_{h,i}(\mathbf{r})|^2.$$

We considered all potentials to be spherically symmetric to simplify the calculations, and when calculating the charge density, the wave functions were averaged over the angle. Then using the Gauss theorem it is possible to write

$$\varphi_{h,i+1}(r) = \frac{e}{\epsilon_0 r}\int\limits_{r'\le r}|\psi_{h,i}(\mathbf{r}')|^2 d^3r'.$$

By way of analogy with [13] we use the three-band Kane's Hamiltonian in the spherical symmetry approximation. Within the framework of this approach, the wave function is represented in a spherical coordinate system as the sum of the basic „angular“ solutions with coefficients depending on the radial coordinate:

$$\psi_M^{(J,L)}(\mathbf{r}) = f_1^{(J,L)}(r)(-i|\Gamma_6, L, J, M\rangle) + f_2^{(J,L)}(r)|\Gamma_8, L+1, J, M\rangle + f_3(r)^{(J,L)}|\Gamma_8, L-1, J, M\rangle \qquad (5)$$

or

$$\psi_M^{(J,L)}(\mathbf{r}) = \begin{pmatrix} -i|\Gamma_6, L, J, M\rangle \\ |\Gamma_8, L+1, J, M\rangle \\ |\Gamma_8, L-1, J, M\rangle \end{pmatrix} \cdot \mathbf{f}^{(J,L)}(r).$$

In this case, the Hamiltonian of a homogeneous semiconductor for given values J and L has the form:

$$\hat{\mathbf{H}}_0^{(J,L)} = \begin{pmatrix} E_g + A_c\hat{K}_-^{(L+1)}\hat{K}_+^{(L)} & P_-\hat{K}_-^{(L+1)} & P_+\hat{K}_+^{(L-1)} \\ P_-\hat{K}_+^{(L)} & -\gamma_+\hat{K}_-^{(L+2)}\hat{K}_+^{(L+1)} & -\nu_2\hat{K}_+^{(L)}\hat{K}_+^{(L-1)} \\ P_+\hat{K}_-^{(L)} & -\nu_2\hat{K}_-^{(L)}\hat{K}_-^{(L+1)} & -\gamma_-\hat{K}_-^{(L)}\hat{K}_+^{(L-1)} \end{pmatrix}, \quad (6)$$

where

$$\hat{K}_+^{(L)} = -\frac{\partial}{\partial r} + \frac{L}{r},$$

$$\hat{K}_-^{(L)} = \frac{\partial}{\partial r} + \frac{L+1}{r}.$$

The material parameters in the Hamiltonian (6) are calculated based on the parameters of the anisotropic four-band Kane's Hamiltonian [15]:

$$P_\pm = P w_\pm^{(J,L)},$$

$$\gamma_\pm = \gamma \pm w^{(J,L)}\nu,$$

$$\nu_2 = \nu w_2^{(J,L)},$$

$$P = \hbar\sqrt{\frac{E_p}{2m_0}},$$

$$A_c = \frac{\hbar^2}{2m_0}\left(1 + 2F + \frac{E_p}{3(E_g+\Delta)}\right),$$

$$\gamma = \frac{\hbar^2}{2m_0}\gamma_1,$$

$$\nu = 2\frac{\hbar^2}{2m_0}\frac{2\gamma_2 + 3\gamma_3}{5},$$

where

$$w_-^{(J,J-1/2)} = \sqrt{\frac{2J+3}{12J}},$$

$$w_+^{(J,J-1/2)} = \sqrt{\frac{2J-1}{4J}},$$

$$w^{(J,J-1/2)} = -\frac{2J-3}{4J},$$

$$w_2^{(J,J-1/2)} = \frac{\sqrt{3(2J-1)(2J+3)}}{4J},$$

$$w_-^{(J,J+1/2)} = \sqrt{\frac{2J+3}{4(J+1)}},$$

$$w_+^{(J,J+1/2)} = \sqrt{\frac{2J-1}{12(J+1)}},$$

$$w^{(J,J+1/2)} = \frac{2J+5}{4(J+1)},$$

$$w_2^{(J,J+1/2)} = \frac{\sqrt{3(2J-1)(2J+3)}}{4(J+1)}.$$

The equations for radial functions will be as follows:

$$\left(\hat{\mathbf{H}}_0^{(J,L)} + e\varphi_0(r)\right)\mathbf{f}_0^{(J,L)}(r) = E_0\mathbf{f}_0^{(J,L)}(r),$$

$$\varphi_{h,0}(r) = 0,$$

$$\left(\hat{\mathbf{H}}_0^{(J,L)} + e\varphi_0(r) + e\varphi_{h,i}(r)\right)\mathbf{f}_{h,i}^{(J,L)}(r) = E_{h,i}\mathbf{f}_{h,i}^{(J,L)}(r),$$

$$\varphi_{h,i+1}(r) = \frac{4\pi e}{\epsilon_0 r}\int_0^r \left|\mathbf{f}_{h,i}^{(J,L)}(r')\right|^2 r'^2 dr'.$$

The scattering matrix method was used in solving these equations with the calculation of the degree of localization of the wave function [13]. Thus, the energies of the ground states of the acceptor with one and two holes were obtained.

It should be remembered that in the case of A_2^0 of the center, the energy of the hole separation does not coincide with the energy E_h in equation (3). Indeed, when one of the particles leaves, its repulsive field ceases to act on the second, which consequently moves to a higher energy level. Thus, if we denote for E_1 the energy of separation of the first hole from the A_2^0-center, and for E_2 — the energy of separation of the second hole from the A_2^{-1}-center, then the energy E_h will be their arithmetic mean:

$$E_h = \frac{E_1 + E_2}{2}.$$

3. Results and discussion

In the course of calculations, we obtained the energy of separation of the first hole from the neutral acceptor and the energy of separation of the second hole from the once ionized acceptor. Calculations were carried out for solid solutions of $Cd_xHg_{1-x}Te$ with a cadmium content of x from 0 to 0.2. This area of compositions covers cases of both inverted and normal zone structure. The temperature was assumed to be zero. The calculation results are shown in Figure 2.

The most interesting is the range of compositions where the energies of separation (capture) of holes with the width of the band gap intersect. Three areas can be distinguished here, which are shown in more detail in Figure 3. In the region (A), the energies of the main acceptor levels lie in the conduction band ($E_g < E_1 < E_2$), and these states are resonant. In region (B), only the deepest state is resonant, and the shallower one is localized ($E_1 < E_g < E_2$). In region (C), both states are localized ($E_1 < E_2 < E_g$).

The system with two localized states ($E_1 < E_2 < E_g$) was discussed in detail in [10,16] in relation to mercury vacancies. The processes of tearing a hole from the A_2^{-1}-center or capturing a hole at the A_2^{-2}-center are similar to those for a single-charge acceptor adjusted for a greater depth of energy levels. The processes of detaching the first hole from the A_2^0-center or capturing the hole at the A_2^{-1}-center are more interesting. When a hole is captured

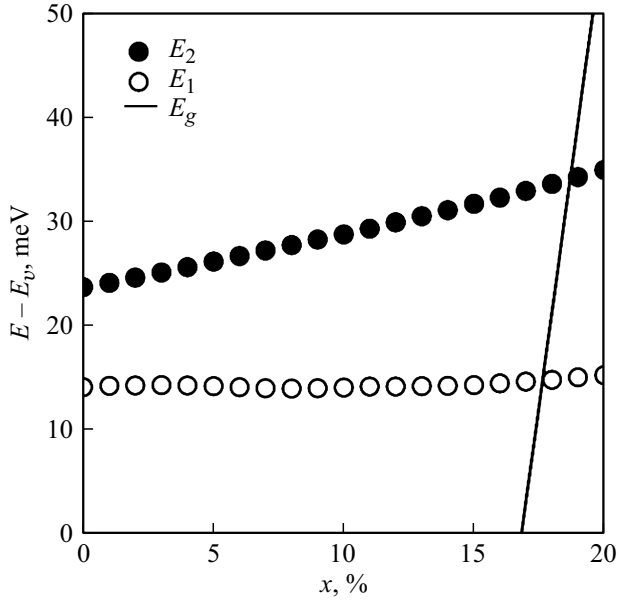

Figure 2. The energy of separation of the first hole from the neutral acceptor (E_1) and the energy of separation of the second hole from a single ionized acceptor (E_2) in solid solutions $Cd_xHg_{1-x}Te$.

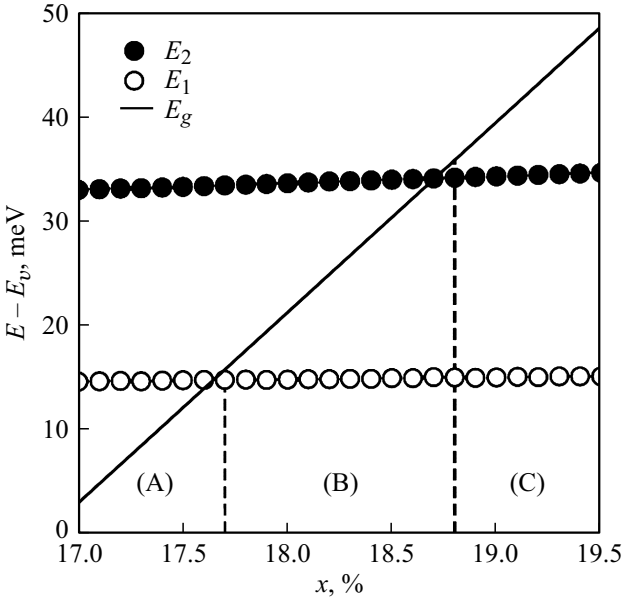

Figure 3. The energy of separation of the first hole from the neutral acceptor (E_1) and the energy of separation of the second hole from a single ionized acceptor (E_2) in solid solutions $Cd_xHg_{1-x}Te$ near the intersection of the energies of localized states with bottom of the conduction band.

by a single ionized divalent acceptor (Figure 4, *a*), an energy equal to E_1 is released, and both holes move to a level with energy E_h. When one hole is detached from the neutral acceptor (Figure 4, *b*), an energy equal to E_1 is consumed, and the remaining hole moves to a deeper level with an energy of E_2.

In narrow-band materials, the bottom of the conduction band is located between the capture energies of the first and second holes ($E_1 < E_g < E_2$), i. e. the deepest state is resonant, or quasi-localized. In this case, the state of the fully ionized acceptor (A_2^{-2}) is unstable. Indeed, we can assume that the conduction band is completely filled with holes, and one of the holes with an energy of E_2 can occupy a deep localized level. In this case, an electron-hole pair is born, and an electron with the same energy E_2 appears in the conduction band. Such resonant levels significantly increase the density of states in the conduction band, and it should be expected that their contribution to photoconductivity and photoluminescence will be very noticeable. Thus, in this system it is possible to observe experimentally both transitions with energy E_1 and with energy E_2.

Finally, consider the case when the bottom of the conduction band is located below the capture energy of the second hole ($E_g < E_1 < E_2$). In this system, in addition to transitions between the lower localized level and the valence band (Figure 4, *a* and *b*), transitions between this level and the conduction band are possible (Figure 4, *c* and *d*). At the same time, the probability of the latter is high, since

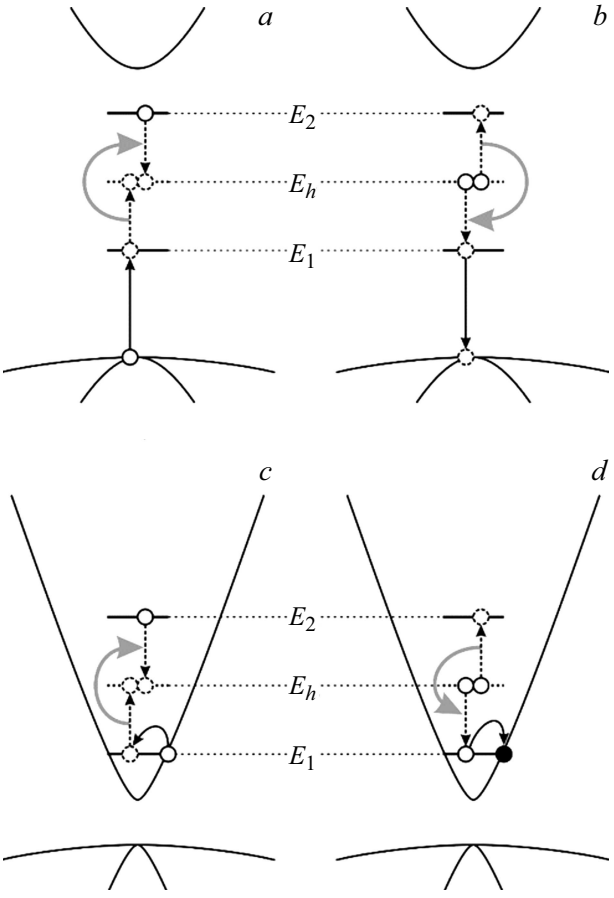

Figure 4. Transition schemes for capturing (a, c) and releasing (b, d) the second hole by a divalent acceptor in the case of localized (a, b) and resonant (c, d) states.

it occurs without changing the energy of the quasi-particles, and the preservation of the quasi-pulse is not required, since the translational symmetry is broken by the acceptor center.

Thus, in such narrow-band materials A_2^{-1}, the centers are unstable due to spontaneous colonization of the lower quasi-localized state by holes from the conduction band (Figure 4, *c*). Therefore, to observe transitions with energy E_2 in such a system, it is necessary to keep a sufficient number of lower resonant levels free due to intense irradiation. From this point of view, solid solutions with a cadmium content of $\sim 15\%$ are more promising than, for example, pure HgTe. Indeed, the calculations performed in [13] show that in $Hg_{1-x}Cd_xTe$, the width of the resonant levels of the single-charge acceptor decreases (and their lifetime increases) with the growth of x. This is due to the fact that, as the distance between the zones with symmetry Γ_6 and Γ_8 decreases at the Γ-point, the proportion of states with symmetry of heavy holes (component f_3 decreases in the conduction band in the expression (5)). At the same time, the intensity of interaction between the deepest acceptor levels (which are tied to the zone of heavy holes) and the states of the continuum of the conduction band decreases. It should be expected that the resonant levels of a two-charge acceptor will have similar properties.

4. Conclusion

A universal method for calculating continuous and discrete spectra based on the scattering matrix method was first used to study the states of a divalent Coulomb acceptor. The energies of the main single-particle and two-particle states (both localized and resonant) were calculated depending on the composition of the solid solution. It was shown that in the case of a resonant two-particle state, the formation of a single-particle state will be unlikely.

Funding

This study was supported by the Russian Science Foundation (grant No. 22-72-10111).

Conflict of interest

The authors declare that they have no conflict of interest.

References

[1] M. Orlita, K. Masztalerz, C. Faugeras, M. Potemski, E.G. Novik, C. Brüne, H. Buhmann, L.W. Molenkamp. Phys. Rev. B, **83**, 115307 (2011).
[2] B.A. Bernevig, T.L. Hughes, S.-C. Zhang. Science, **314**, 1757 (2006).
[3] M. König, S. Wiedmann, C. Brüne, A. Roth, H. Buhmann, L.W. Molenkamp, X.-L. Qi, S.-C. Zhang. Science, **318**, 766 (2007).
[4] M. Orlita, D.M. Basko, M.S. Zholudev, F. Teppe, W. Knap, V.I. Gavrilenko, N.N. Mikhailov, S.A. Dvoretskii, P. Ne-gebauer, C. Faugeras, A.-L. Barra, G. Martinez, M. Potemski. Nature Physics, **10**, 233 (2014).
[5] A. Rogalski. Opto-Electron. Rev., **20**, 279 (2012).
[6] S.V. Morozov, V.V. Rumyantsev, M.A. Fadeev, M.S. Zholudev, K.E. Kudryavtsev, A.V. Antonov, A.M. Kadykov, A.A. Dubinov, N.N. Mikhailov, S.A. Dvoretsky, V.I. Gavrilenko. Appl. Phys. Lett., **111**, 192101 (2017).
[7] K.E. Kudryavtsev, V.V. Rumyantsev, V.V. Utochkin, M.A. Fadeev, V.Ya. Aleshkin, A.A. Dubinov, M.S. Zholudev, N.N. Mikhailov, S.A. Dvoretskii, V.G. Remesnik, F. Teppe, V.I. Gavrilenko, S.V. Morozov. J. Appl. Phys., **130**, 214302 (2021).
[8] V.V. Rumyantsev, D.V. Kozlov, S.V. Morozov, M.A. Fadeev, A.M. Kadykov, F. Teppe, V.S. Varavin, M.V. Yakushev, N.N. Mikhailov, S.A. Dvoretskii, V.I. Gavrilenko. Semicond. Sci. Technol., **32**, 095007 (2017).
[9] V.V. Rumyantsev, S.V. Morozov, A.V. Antonov, M.S. Zholudev, K.E. Kudryavtsev, V.I. Gavrilenko, S.A. Dvoretskii, N.N. Mikhailov. Semicond. Sci. Technol., **28**, 125007 (2013).
[10] D.V. Kozlov, V.V. Rumyantsev, A.M. Kadykov, M.A. Fadeev, N.S. Kulikov, V.V. Utochkin, N.N. Mikhailov, S.A. Dvoretsky, V.I. Gavrilenko, H.-W. Hübers, F. Teppe, S.V. Morozov. Pisma ZhETF **109**, 679 (2019). (in Russian).
[11] M.S. Zholudev, D.V. Kozlov, N.S. Kulikov, A.A. Razova, V.I. Gavrilenko, S.V. Morozov. FTP, **54**, 695 (2020). (in Russian).
[12] M.S. Zholudev, V.V. Rumyantsev, S.V. Morozov. FTP, **55**, 391 (2021). (in Russian).
[13] M.S. Zholudev, V.V. Rumyantsev, S.V. Morozov. Semicond. Sci. Technol., **37**, 025003 (2022).
[14] M.S. Zholudev, V.V. Rumyantsev, S.V. Morozov. Pisma ZhETF **116**, 307 (2022). (in Russian).
[15] E.G. Novik, A. Pfeuffer-Jeschke, T. Jungwirth, V. Latussek, C.R. Becker, G. Landwehr, H. Buhmann, L.W. Molenkamp. Phys. Rev. B, **72**, 035321 (2005).
[16] D.V. Kozlov, T.A. Uaman Svetikova, A.V. Ikonnikov, V.V. Rumyantsev, A.A. Razova, M.S. Zholudev, N.N. Mikhailov, S.A. Dvoretsky, V.I. Gavrilenko, S.V. Morozov. Pisma ZhETF **113**, 399 (2021). (in Russian).

Translated by A.Akhtyamov